

JUN 0 8 1988

3003.1/MB/88/05/19

- 1 -

MEMORANDUM FOR: Ronald L. Ballard, Branch Chief  
Technical Review Branch, DHLWM

THRU: Philip S. Justus, Section Leader  
Geology/Geophysics Section, HLTR

FROM: Michael E. Blackford  
Geology/Geophysics Section, HLTR

SUBJECT: 1988 SPRING MEETING OF THE AMERICAN GEOPHYSICAL UNION  
MEETING

LOCATION: Baltimore Convention Center, Baltimore, Maryland

DATE OF TRIP: May 17, 1988

BACKGROUND AND PURPOSE OF TRIP:

The American Geophysical Union annually holds two meetings, one in the fall in San Francisco, California, and one in the spring in Baltimore, Maryland. These meetings enable scientists of many disciplines to come together and present papers on their work. More than a dozen different disciplines are represented including atmospheric sciences, geodesy, geomagnetism, paleomagnetism, hydrology, seismology, tectonophysics, volcanology, geochemistry, and petrology, which may have sessions of interest to the high-level waste management program.

The purpose of my attendance at the meeting was to keep abreast of some of the current studies in the field of seismology. I also attended a presentation by Joel Grimm of the Division of Low-Level Waste and Decommissioning entitled, "Regulatory Perspective on Geomorphic Stability at Waste Disposal Sites During Extreme Rainfall Events."

SUMMARY OF PERTINENT POINTS:

There were two sessions under the discipline of seismology on May 17. The morning session dealt with the topic of earthquake parameters and consisted of eleven presentations. The afternoon session was concerned with earthquake rupture processes and there were seven papers presented. The first paper of the session was withdrawn. Abstracts of papers are attached to this report.

SUMMARY OF ACTIVITIES:

In addition to my attendance at the sessions described above, and to my attendance at the presentation by Joel Grimm, I attended the AGU Seismology Section Luncheon. The luncheon speaker gave a summary report on a recent

8806080396 880603  
PDR WASTE  
WM-1 DCD

NH18  
delete T255  
302

Wm-1

workshop held at Woods Hole, Massachusetts on the current state of ocean bottom seismography.

NRC STAFF IMPRESSIONS:

In general the presentations were quite good and showed an adequate degree of preparation. Of particular personal interest was a paper by Adam Dziewonski and others on the earthquake sequence in the Gulf of Alaska in November 1987. The sequence included two earthquakes in the upper 7.0 magnitude range. Dziewonski presented a number of centroid-moment tensor solutions and aftershock seismicity plots that indicate that the sequence occurred on a previously unrecognized north-south oriented structure. He did not, however, offer a hypothesis reconciling this activity with the general concept of tectonics in the area.

Another paper of the morning session, which may have some implications for HLW, was a paper on the Tennant Creek, Australia earthquakes of January 1988 by J.R. Bowman and others. The largest of the earthquakes, of a size similar to the 1983 Borah Peak, Idaho earthquake, had a similar surface rupture pattern. These earthquakes were apparently the result of movement on a thrust fault in contrast to the normal faulting associated with the Borah Peak earthquake. Also the presenter did not mention any hydrologic effects of the type observed in the Borah Peak macroseismic zone.

Finally a paper by Harold Patton of Lawrence Livermore National Laboratory on earthquake mechanisms in northern California and the northern Great Basin in Nevada brought into focus the contrast between earthquake mechanisms in the northern Great Basin and the southern Great Basin. Northern Great Basin mechanisms tend to be of the normal type, while southern Great Basin mechanisms are typically strike-slip in nature. The component of least compressive stress is nearly horizontal and oriented roughly E-W in both segments of the Great Basin while the component of most compressive stress is roughly vertical in the northern Great Basin and horizontal in the southern Great Basin. Patton speculated that this contrast may be related in some way to the subducted Gorda tectonic plate.

REFERENCES:

See the attached abstracts for the Tuesday, May 17, Seismology Section and Hydrology Section sessions.

15/

Michael E. Blackford  
Geology/Geophysics Section, HLTR

OFC	:HLTR	WLB	:HLTR	:	:	:	:	:
NAME	:MEBlackford	:PSJustis	:	:	:	:	:	:
DATE	:88/06/01	:88/06/02	:	:	:	:	:	:

DISTRIBUTION

Central File	NMSS RF	RBrowning, HLWM	JBunting, HLSE
BYoungblood, HLOB	MBlackford, HLTR	PJustus, HLTR	HLTR RF

OFC: HLTR	:HLTR	:	:	:	:	:
NAME:MEBlackford:PSJustus:	:	:	:	:	:	:
DATE: 88/06/01	:88/06/02:	:	:	:	:	:

# Earthquake Parameters (S21)

## Room 310 Tues AM

### Presiding, A. A. Barka

#### MIT

#### B. W. Tichelaar

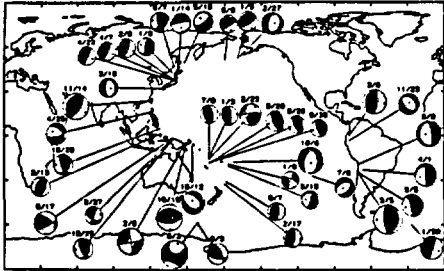
#### Univ of Michigan

S21-01 0830H  
Global Seismicity of 1987.

G. ZWART, A. M. Dziewonski, G. Ekström<sup>1</sup> and J. H. Woodhouse (Department of Earth and Planetary Sciences, Harvard University, Cambridge, Ma. 02138)

We continue our systematic analysis of source mechanism of current earthquakes; 673 centroid-moment tensor (CMT) solutions were obtained through the end of October. It is expected that the total for the entire year will approach 800. The map below shows the events with magnitude  $M_w \geq 6.5$  from November 1986 through October 1987. The radius of a baseball is a linear function of magnitude. The moment tensor solutions are shown by shading; continuous lines represent best double couple solutions.

During the last year we have completed the analysis of events recorded by the global digital networks since January 1, 1977. There exists now a catalog of 6,700 CMT solutions for the 11 year period with a uniform threshold of, roughly,  $1 \times 10^{24}$  dyne-cm.



<sup>1</sup> Now at Lamont-Doherty Geological Observatory, Palisades, N.Y.

S21-02 0845H  
Rupture Initiation of the Great 1960 Chilean Earthquake

BRIAN P. COHEE and LARRY J. RUFF (Department of Geological Sciences, University of Michigan, Ann Arbor, MI 48109)

The 22 May 1960 Chilean subduction event, the largest magnitude earthquake ( $M_w = 9.5$ ), provides an opportunity to investigate the rupture process of an exceptionally large (estimated  $800 \times 200$  km<sup>2</sup>) fault surface. A striking characteristic of this event is the foreshock sequence with three  $M_w \geq 7.5$  foreshocks, occurring 33 hr, 9 hr, and 15 min before the mainshock, unfortunately the last foreshock obscures the arrival of the mainshock P wave.

Foreshock depths are determined using  $pP$ - $P$  times identified on seismograms recorded by the Caltech broadband 1-90 instrument at Palomar. Moment rate functions are then deconvolved from the foreshock P waves; we are able to constrain the focal mechanisms to be shallow-dipping thrust. The last foreshock 15 min prior to the mainshock is coincident with the beginning of an unusually long-period (300-600 s) precursor observed by Kanamori and Cipar on the Benioff strain seismogram at Pasadena. Although body wave deconvolution will not be sensitive to this ultra-low frequency moment release, we can test whether the rupture history was anomalous in the long-period P wave band. We find the moment rate function of the last foreshock to be a simple pulse with 10-15 s duration, typical for an underthrusting event of this magnitude. Furthermore, the simple rupture history, fault geometry and depth of this last foreshock are nearly identical to the large foreshock 9 hr earlier. The similarity of both events is clear when the waveforms are compared, particularly at IGY station TSK (Az= 277°) which is not sensitive to the  $\approx 50$  km N-S separation of the two foreshocks. The equivalence of these two foreshocks allows the last foreshock to be subtracted from the mainshock seismogram. The first 15 min of the two foreshock traces are cross-correlated to yield the optimum time shift and scaling factor, then the continuation of the earlier foreshock is subtracted from the combined last foreshock plus mainshock trace. The residual seismogram illustrates the awesome nature of the mainshock; the long-period body wave amplitudes steadily increase for more than 8 min before going off-scale.

S21-03 0900H  
Depth of Seismic Coupling in the Chilean and Northern Honshu Subduction Zones

Bart W. Tichelaar and Larry J. Ruff (Department of Geological Sciences, The University of Michigan, Ann Arbor, MI 48109)

Underthrusting at subduction zones can cause large earthquakes at shallow depths, but is always accommodated by aseismic creep below a certain depth. This transition depth is an important component of seismic coupling and can be characterized as the maximum depth of rupture extent of the deepest underthrusting earthquakes. It is thus important to determine the maximum

depth of significant moment release for those interplate events that occur furthest landward from the trench axes. Using this criterion, we have studied four events in the central Chilean subduction zone between 25 and 35°S (28 Dec 66  $M_w=7.5$ , 4 Oct 83  $M_w=7.3$ , 26 Sep 67  $M_w=6.0$  and 4 Mar 85  $M_w=6.0$ ), one in northern Chile (21 Dec 67  $M_w=7.4$ ) and the 12 June 87  $M_w=7.5$  Miyagi-Oki earthquake in northern Honshu. The smaller earthquakes can be considered as point sources and depths are determined by picking depth phases as observed on long period WWSSN records. For the larger earthquakes, the time separation between direct P and depth phases can be shorter than the source duration, which makes it difficult to identify depth phases. In these cases, the lower depth extent of significant moment release is obtained by deconvolving source time functions from long period WWSSN P waves.

Rupture of the central Chilean earthquakes does not go deeper than 40±5 km, which indicates that the subduction zone is seismically decoupled below this depth. The 4 Mar 85 event is located at the downwind edge of the mainshock rupture area (3 Mar 85  $M_w=8.2$  Chilean earthquake), which implies that the maximum depth extent of the mainshock is 40 km. The 1978 Miyagi-Oki earthquake occurred in a subduction zone where the subducting lithosphere is much older than in central Chile, yet the lower depth extent of significant moment release is 40±5 km, the same depth as in central Chile. There are indications that the northern Chile earthquake has a depth extent resolvable deeper than 40 km. This suggests that northern Chile may be an anomalous region with a deeper coupled zone.

S21-04 0915H  
Source Duration and Depth Extent of the June 22, 1977 Tonga Earthquake

Jiann Zhang and Thorne Lay (Department of Geological Sciences, University of Michigan, Ann Arbor, MI 48109)

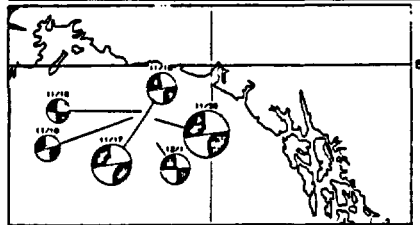
The June 22, 1977 Tonga earthquake has the longest source duration ever reported for a normal-fault earthquake. The 150 km depth range spanned by aftershocks of the earthquake is also unusually large. There has been substantial controversy over both the depth extent of rupture and the source duration for this earthquake. We study the long-period characteristics of the source process of the Tonga event using long-period Rayleigh waves recorded at IDA and GDSN stations. A well-resolved source duration of  $84 \pm 3$  sec is obtained using a least-squares inversion method. We use the spectral amplitude as a weighting factor in measuring the misfit between the data and a given source finiteness model. The introduction of this weighting reduces the scatter and improves the resolution of the source duration determined from data ranging in period from 150 to 300 sec. The results indicate that the temporal variation of the moment rate tensor of the earthquake is small, and suggest that the long-period component of stress release of the earthquake is smooth. The horizontal and vertical source directivity cannot be determined with confidence. However, the centroid depth of the earthquake is well resolved at 90 km with 90% confidence range (70, 100) km. The estimated error in the depth determination due to the uncertainties in the source finiteness and earth models is quite small. The results indicate that the rupture of the earthquake excites long-period seismic waves at depths somewhat deeper than the depth of 70 km determined from the first arrival waves. Inversion for the vertical rupture extent indicates that the rupture propagates down to 107 km depth for an uniformly distributed source starting at 75 km depth, and to 150 km for a source starting from 40 km depth. The fundamental Rayleigh waves with periods longer than 150 sec cannot resolve which vertical extent of faulting is more appropriate.

S21-05 0930H  
November 1987 Sequence in the Gulf of Alaska.

A. M. Dziewonski, G. Ekström<sup>1</sup> and G. Zwart (Department of Earth and Planetary Sciences, Harvard University, Cambridge, Ma. 02138)

Centroid-moment tensor (CMT) solutions were obtained for six events in the Gulf of Alaska; there is no record of previous seismicity in this area. The eigenvalues and eigenvectors of the full solution are listed below. There is the usual for shallow events instability with respect to the  $M_{11}$  and  $M_{22}$  components. The map shows solutions obtained with these two elements set to zero. The methods of very-broad-band analysis (Ekström, 1987) are employed to obtain the source time function and the directivity vector.

Date and Time	Nov 17 0846:	Nov 18 0618:	Nov 18 0713:	Nov 18 1301:	Nov 30 1923:	Dec 1 1203:
Scale factor	$10^{26}$	$10^{24}$	$10^{25}$	$10^{24}$	$10^{27}$	$10^{24}$
T Value	6.9	1.2	3.9	5.7	7.9	5.4
T Plunge	19°	16°	3°	1°	4°	5°
T Azimuth	124°	114°	139°	309°	309°	313°
N Value	-0.6	0.1	0.1	-0.3	0.4	0.0
N Plunge	56°	53°	75°	86°	70°	82°
N Azimuth	4°	359°	241°	90°	51°	75°
P Value	-6.3	-1.3	-4.0	-3.2	-6.3	-5.4
P Plunge	27°	30°	14°	3°	19°	7°
P Azimuth	224°	214°	48°	219°	217°	222°



<sup>1</sup> Now at Lamont-Doherty Geological Observatory, Palisades, N.Y.

S21-06 0945H  
The Alaskan Earthquakes of November 17 and 30, 1987: Very Long Period and Broad Band Analysis of Quasi-Real Time Tele-transmitted Geoscope Data.

A. Deschamps, P. Bernard, M. Bezeghoud, T. Monfret, S. Romanowicz (all at Laboratoire de Sismologie, Institut de Physique du Globe de Paris, 4 place Jussieu, 75252, Paris cedex 05, France). (sponsor B. Romanowicz)

Within a few days of the occurrence of the  $M_w=7.9$  Alaskan earthquake of November 30, 1987, we were able to obtain a preliminary estimate of moment, source parameters and source time functions based on very long period and broad band data from 9 GEOSCOPE stations, linked to Paris by teletransmission via phone lines. These results were presented on a crash poster at the San Francisco Fall AGU meeting and have been confirmed since in a new detailed study.

GEOSCOPE very long period data were inverted to determine seismic moment ( $M_w = 0.4 \times 10^{26}$  Nm), source duration ( $\tau/2 = 20$  s), directivity ( $N170^\circ E$ ), and source mechanism (a surprising strike slip in a north-south direction). The directivity towards the south is in good agreement with the aftershock zone (as reported by USGS) which also permits to choose the N-S nodal plane as the rupture plane. This event appears to be one of the largest strike-slip events ever recorded related to an intracontinental feature.

Broad band records of P waves at 7 GEOSCOPE stations located in the appropriate distance range have been inverted to obtain the individual source time functions, with a depth fixed at 20 km. The source duration is 30-40 s, and station SBB is the only one where complexity is resolved into three 10 seconds sources, due to its location in the direction opposite to that of rupture propagation. The seismic moment found is generally smaller than that obtained at very long periods.

The November 17 precursor has also been studied in a similar way. The mechanism is slightly more dip-slip than that of the main event, the moment about 10 times smaller, and the source is composed of a main part of duration 20s and a second smaller source.

S21-07 1020H  
Seismicity, Focal Mechanisms and Tectonics Related to Three 1986 Earthquakes in the Vicinity of Taiwan

D. Salzberg, F. Wa, J. Barker (Dept. Geol. Sc., SUNY Binghamton, NY 13901), R. McCaffrey (M.I.T.), J. Wang, and K. C. Chen (Acad. Sin. Taiwan, ROC)

Three significant earthquakes occurred in the vicinity of Taiwan in 1986 as shown below. Event 1 was located near the southern terminus of the Okinawa Trough, east of the Ilan plain of northeastern Taiwan. Events 2 and 3 took place in areas contiguous to each other, near the northern end of the Longitudinal Valley (LV), which is at the junction of the collision boundary between the Philippine Sea and the Eurasian plates. Two different body wave inversion methods were used to derive focal mechanism for events 1 and 2, and the results obtained agree within the data resolution. Event 3 is being studied.

#	mmdd	Long.	Lat.	Str.	Dip	Strike	Rake	$M_0$ (dy-cm)	h(km)	Note
1	0116	122.01	24.77	39	39	162	1.1x10 <sup>26</sup>	8		
2	0520	121.62	24.13	47	43	107	2.6x10 <sup>26</sup>	19		
3	1114	121.57	23.90	43	35	100	9.3x10 <sup>26</sup>	33	PDE	

The initial aftershocks of event 2 defined an inclined zone striking  $N45^\circ E$  and dipping  $45^\circ$  toward the SE which coincides with the SE dipping plane of the inversion results. These initial aftershocks were followed by a series of shallow shocks above the dipping zone and event 3 occurred almost six months later in a zone less than 10km away. The thrust mechanisms of events 2 and 3 together with similar mechanism for the 1972  $M_w=7.2$  earthquake calls for a reevaluation of the motion along the LV. So far no verifiable strike-slip solution has been identified for  $M>5.5$  earthquakes associated with the LV. The NE striking normal fault event associated with event 1 agrees well with the tensional nature of the Okinawa Trough and the Ilan plain. It is also consistent with other earthquakes in the same area.

S21-08 1035H  
Tennant Creek Earthquakes of 22 January 1988: Reactivation of a Fault Zone in the Proterozoic Australian Shield

J. R. Bowman (Research School of Earth Sciences, Australian National University, GPO Box 4, Canberra, ACT 2601)  
T. Jones (Bureau of Mineral Resources, GPO Box 378, Canberra, ACT 2601, Australia)  
G. Gibson and A. Corkin (Seismology Research Centre, Phillip Inst. of Technology, Plenty Road, Bundoora, Vic. 3083.)  
R. Thompson and A. Camacho (Northern Territory Dept. of Mines and Energy, PO Box 2635, Alice Springs, NT 5750)

Three  $M_w$  6.5-7.0 earthquakes occurred 30 km southwest of Tennant Creek in the Northern Territory of Australia on 22 January 1988 at 00:36 UT ( $M_w$  6.5), 03:57 ( $M_w$  6.7) and 12:05 ( $M_w$  7.0). The third event of this series was of size at least comparable to the largest earthquakes on the Australian continent during this century and produced a surface rupture extending 28 km. There is no historic or instrumental record of earthquakes larger than magnitude 5 within 500 km of these events prior to 1987. Records from the WRA seismic array, situated 30 km east of the ruptures, show no obvious signs of local seismic activity between 1964 and late 1985. In late 1985 a sequence of small ( $M_w < 4.3$ ) earthquakes began, which culminated in two  $M_w$  5.2 earthquakes in January 1987. The zone of aftershocks of the 1987 events coincides with the 1988 surface ruptures.

Low magnitude activity continued through 1987. The main fault scarp trends WNW for 15 km before bending to a WSW orientation and extending another 8 km. A second WNW trending scarp segment of 7 km length is located on the extension of the WNW portion of the main fault but separated by a 7 km gap exhibiting no disturbance. Surface deformation on the WNW trending scarps generally consists of an asymmetric bulge of up to 1.5 m height with the south side high and a north facing scarp of up to 0.6 m suggesting south over north thrusting. Deformation on the WSW segment is more variable. A gas pipeline crossing the fault zone was kinked and indicates shortening by 1.9 m. Displacement of fences indicates primarily thrusting combined with 0.4 cm of left lateral motion. The WNW sections of the fault follow lineations in aerial photographs, while the WSW arm of the main fault is colinear with a quartz ridge which is locally mylonitized. Both of these observations suggest that reactivation of a Proterozoic fault produced the 1985 earthquakes.

S21-09 1050H

Seismic Gap in the Eastern Part of the North Anatolian Fault Zone

A. A. Barka and M. N. Toksoz (Earth Resources Lab, Department of Earth, Atmospheric, and Planetary Sciences, M.I.T., Cambridge, MA 02139)

Historical and instrumental earthquakes in the eastern part of the North Anatolian fault zone between the Eriçan pull-apart basin and the Karlıova triple junction where the North and East Anatolian fault zones intersect, have been examined in relation to fault segmentation. Results of this study suggest that each rupture segment may have its own characteristic earthquakes. The westward migration of six large earthquakes between 1939 and 1967 has created a continuous surface break from the east end of the Eriçan pull-apart basin to the west end of the Madurua valley. To the east of the Eriçan pull-apart basin, however, there is another westward migration of large earthquakes. This migration consists of two rupture segments. The eastern rupture segment has last ruptured in 1949 ( $M=6.7-7$ ) and it has restraining double bend geometry. The western rupture segment of this eastern migration appears to be a seismic gap. This segment extends between the Yedigöller and Eriçan pull-apart basins for a total length of 76 km; it has last ruptured in 1784 by an earthquake of intensity IX. The 1967 moderate earthquake ( $M=5.6-6.2$ ) occurred along its most eastern fault segment and created 20 cm right-lateral surface displacement. Recurrence intervals of historical earthquakes and geological data indicate that the slip rate in this part of the fault zone is about 1 cm/yr. This results in the accumulation of about 3 m right slip along the western part of the 1784 rupture segment. The two separate sequences of westward migration of large earthquakes along the North Anatolian fault zone is due to the fact that the eastern part of the westward escaping Anatolian block has divided into two wedge shaped blocks southeast of the Eriçan pull-apart basin, each of which moves relative to each other.

S21-10 1105H

Earthquake Mechanisms in Northern California and Northwestern Great Basin and Their Implications to the Regional Stress Field

H. J. Patton (University of California, Lawrence Livermore National Laboratory, P. O. Box 808, Livermore, California); 415-422-3924

We are studying the source mechanisms of earthquakes in northern California and across the Cascades into the Great Basin of northern Nevada for new information on the regional stress field and on the influence that the North America-Pacific plate boundary has on the style of faulting associated with basin and range formation. The earthquakes have magnitudes between four and five, and their mechanisms were determined by moment-tensor inversion of intermediate-period, 40-10 sec, surface waves recorded in western United States. The inversion also returns an independent estimate of the focal depth. Waveform data is taken from the Global Digital Seismographic Network and Livermore's digital NTS network, along with hand-digitized MMSN records. To date, we have analyzed five events in northern California and several events in the Great Basin. Four of the five events in California show tension axes horizontal and oriented ENE-WSW to due E-W. We have also analyzed one event which gave a depth near 35 km and is apparently in the Gorda Plate beneath northern California. Its mechanism shows a large strike-slip component and appears to be consistent with the results of Walter (1986). Normal faulting seems to prevail in the Cascades and across into the northern Great Basin.

S21-11 1120H

Corrections to the Surface-Wave Magnitudes Based on the Old Albany Bosch-Onceri Seismographs

M. Mitrovic (NYS Geological Survey, CEC, State Education Department, Albany, NY 12230; 518-484-2021)

Two Bosch-Onceri seismographs (N-S and E-W comp.) were operated by the New York State Geological Survey in Albany, New York from March 1906 through September 1912, at a time when very few seismic instruments of any type were in operation in the world. Until recently, the only known information on calibration for the station was that the natural period ( $T_0$ ) of both instruments was 30 sec and the static magnification (gain) 10 to 12 times. Assuming that the effective gain at  $T=20$  sec was equal to the static gain of 12 times, I have calculated one-station, surface-wave magnitudes ( $M_0$ ) for 56 large earthquakes from around the world as recorded at Albany by these instruments (Albany

catalog). These magnitudes agreed, on the average, to those from the best current catalog of all known world earthquakes for 14 shallow events in common to both catalogs, even though no corrections were made for the effects of extreme underdamping on effective gain and its dependence on signal amplitude for these instruments. Analysis of calibration data, found since those calculations were made, suggests that the Albany Bosch-Onceri instruments were highly underdamped and that the damping parameter ( $h$ ) depended on signal amplitude as recorded on smoked-paper seismograms ( $h$  increased with decreasing amplitude). If  $T_0$  of such an instrument is close to the period of surface waves used in determining  $M_0$  (20 sec), it becomes difficult to estimate  $M_0$  accurately because the true gain near  $T_0$  is very sensitive to small variations in  $T$  and signal amplitude. For the Albany instruments, however, the effective gain near 20 sec can be determined quite accurately (1.8 times the static gain.) Gain is not amplitude dependent, even though  $h$  is, because the  $T_0$  (30 sec) was substantially larger than 20 sec. This correction for the effective gain, relative to the static gain, removes the average observed discrepancy in the Albany  $M_0$  (0.25 units) for all surface wave amplitudes except the very smallest. The additional effect of "free" (dead) play of a few millimeters in the complex mechanical recording pen on the effective gain of these seismographs accounts well for the remaining discrepancy in the Albany  $M_0$  at the smallest signal amplitudes.

## Earthquake Rupture Processes (S22)

Room 301 Tues PM  
Presiding, G. C. Beroza  
MIT  
P. G. Okubo  
USGS, Menlo Park

S22-01 1400H

Rupture Propagation in a Nonuniform Stress Field Following a State Variable Friction Model

Paul G. Okubo (U.S. Geological Survey, 345 Middlefield Road, Menlo Park, CA 94025)

Over roughly the past decade, much of the research in experimental rock mechanics has been focused on the state variable frictional constitutive relation of the kind introduced by J.H. Dieterich and further developed by A.L. Ruina and others. This rate- and state-dependent friction constitutive formulation accounts for a range of laboratory observations of rate-dependent sliding behavior and it allows for fault restrengthening by means of a time-dependent-like effect. Some workers suggest that state variable friction fault models might be preferred over fault models that contain explicitly displacement-dependent fault weakening constitutive relations. Numerical simulations and theoretical analyses have demonstrated the versatility of the state variable models. They have also been shown to be capable of accounting for laboratory observations of dynamic frictional sliding or stick-slip.

A state variable friction fault model has been included in a numerical model for dynamic Mode II shear crack calculated using a boundary integral method. By using the same fault constitutive relation in both quasistatic and dynamic calculations, the complete fault slip history from stable nucleation through dynamic rupture propagation is simulated. First a quasistatic model is calculated to a point leading to fault instability; the results from this calculation are used to specify the initial conditions for the dynamic model. Then, rupture models for dynamic fault propagation from a high-stress patch into a low-stress patch are calculated. The ruptures propagate at the Rayleigh wave speed after nucleation. The rupture front decelerates when it reaches the edge of the high-stress patch and propagates beyond this, depending on the size of the stress difference between the two patches. The amount of rupture overshoot into a region of negative dynamic stress drop also depends on the high-low stress difference.

S22-02 1415H

Short Period Acceleration from a Stochastic Fault Model and Constraint on the Fault Heterogeneities

Junji KOYAMA (Geophysical Institute, Faculty of Science, Tohoku University, Sendai 980 Japan)

A stochastic fault model is considered to describe the heterogeneous faulting of large earthquakes. Radiation of short waves is related to the random fracture of small scale fault heterogeneities (random fault patches). The random fault patches are represented by the variance of local stress drop,  $\Delta\sigma^2$ , and by the rupture time of a characteristic patch size,  $l/\lambda$ . Seismic directivity effect on the amplitude of short waves is also derived from the model, which is different from the seismic Doppler effect on the long waves. The excitation of short period acceleration is formulated by the stochastic parameters of the fault patches and overall fault size,  $L$  and  $W$ , in addition to the short-period seismic directivity effect.

Since the seismic intensity is relevant to the strength of acceleration, we could retrieve the information on the fault heterogeneities from

the size of isoseismals of large earthquakes. Maximum acceleration is scaled by the source terms as  $(W^3/L\lambda^2\Delta\sigma^2)^{1/2}$  excluding directivity and propagation effects. A relation between maximum acceleration and seismic moment is obtained from large earthquakes in Japan and China as  $M_0 \propto (\Delta\sigma_0/L\lambda^2\Delta\sigma^2)^{1/2}$ . This leads to  $\lambda^2\Delta\sigma^2 \propto \Delta\sigma_0 L^2 W^3$ , where  $\Delta\sigma_0$  is average stress drop on the fault.  $\lambda^2$  is patch corner frequency and it corresponds to the number density of random fault patches within a unit fault area. Therefore, the latter relation means that the fluctuation of local stress drop within a unit fault area is invariant independent of earthquake source sizes.

S22-03 1430H

Dynamic Fracture Propagation using the Finite Element Method

D V Swenson (Mechanical Engineering Dept., Kansas State University, Manhattan, KA 66506; 913-532-5610)  
J.C. DeBorja (Dept. of Geology and Geophysics, Rice University, Box 1892, Houston, TX 77251; 713-527-4886)

We are modelling the rupture process on either new or pre-existing fractures by the finite element method. This presents the following advantages, many of which cannot be obtained by any other method: 1. Any number of materials may be present; they can have any geometry. 2. The crack may propagate in any direction, rather than only along grid lines. 3. Remeshing is automatic. 4. The energy balance is computed at every time-step. 5. Interface elements may be inserted to simulate fault gouge. 6. The stress singularity at the crack tip is included.

Since the wave equation is solved at every time step, synthetic seismograms are obtained, and can be displayed for any point in the domain. Plots of the deformed mesh or any part thereof can be made. The code also includes warnings that the stress initiation has been exceeded, and that a new crack must be initiated. While the present code only treats two-dimensional problems, it could be extended to three dimensions if this were warranted.

An early application of the method showed the head-on propagation of two cracks, followed by their avoidance, attraction, and by the final separation of the domain, a process which is duplicated by the formation of overlapping spreading centers along mid-oceanic ridges. Other problems of geophysical interest will be discussed.

S22-04 1445H

Insights Into Creep, Afterslip, and Triggered Slip From Numerical Simulation

R.L. Wesson (U.S. Geological Survey, MS 922 National Center, Reston, VA 22092)

Observations of fault creep, afterslip, and triggered slip along active faults and analytic and numerical studies of the dynamics of fault creep suggest the following: 1) the long-term creep rate (or afterslip rate) at a point along an active fault is controlled by the long-term loading rate and by the geometric distribution of stuck and creeping areas on the fault zone, 2) individual, simple creep events represent the failure of discrete "creep asperities," 3) more complicated creep events represent the interaction and successive failure of multiple "creep asperities," 4) the amplitude of a creep event is proportional to the yield stresses of the asperities involved, 5) the rise time of an individual event is proportional to the yield stress of the asperity and the local rheological properties of the creeping fault, and 6) afterslip and triggered slip are fundamentally the transient response of the weak, creeping, portions of the fault zone to changes in the static stress field resulting from the sudden, deep-seated, dislocation that caused the preceding earthquake. Thus, creep is a fundamental process that acts to redistribute and concentrate changes in stress, from either long-term loading or nearby earthquakes, onto the stuck portions of the fault that fail only in earthquakes. Inasmuch as episodes of creep, afterslip, and triggered slip are periods of relatively rapid stress increase on the stuck portions, these intervals of time should be regarded as periods of higher earthquake probability in the affected areas.

S22-05 1530H

EARTHQUAKE STRAIN STEPS, SEISMIC MOMENT AND TOTAL EARTHQUAKE MOMENT

M. J. S. Johnston (U.S.G.S., Menlo Park, CA, 94025)  
A. T. Linde (DTM, Washington, D.C., 20015)  
G. D. Myren (U.S.G.S., Menlo Park, CA, 94025)

The static strain field generated by an earthquake provides a simpler diagnostic of the seismic source parameters than that derived from spectra of the radiated seismic waves. Co-seismic strain offsets have been recorded for 17 earthquakes since 1982 on clusters of Sacks-Everston deep borehole strainmeters installed along the San Andreas fault. These strain offsets, which occur only during nearby moderate to large magnitude earthquakes, agree well with, or perhaps slightly exceed, the static strain field steps calculated from simple elastic half-space dislocation models of these earthquakes, scaled by their seismic moment. Since the strain steps result from total fault slip (i.e. the slip contributing to dynamic seismic radiation and any seismic fault slip), the moment contributing to the step is known as the total seismic moment. Total seismic moment determinations are therefore simply and routinely made from step observations recorded with the present limited strainmeter arrays and earthquake location and focal mechanism data. At particular locations, where the strainmeter clusters are more comprehensive or optimally placed, constraints on other seismic source parameters can be made.

S22-05 1545H

Searching for "Slow" and "Silent" Earthquakes Using Free Oscillations

GREGORY C. BEROZA and THOMAS H. JORDAN (both at Dept. of Earth, Atmospheric, and Planetary Sciences, M.I.T., Cambridge, MA, 02139)

Our knowledge of earth structure can be used to distinguish far-field seismic signals from near-field noise. An earthquake will excite ground motion at the eigenfrequencies of the Earth's normal modes. By calculating the energy in small bands centered on the known frequencies of the normal mode peaks, and comparing it to the energy in adjacent noise bands, it is possible to detect earthquakes at low frequencies without knowing anything about them at high frequencies. We have developed an earthquake detection algorithm that compares the zeroth-order moment of the mode bands with that of the noise bands by a chi-squared test. The excitation of each mode at all stations and of the level of excitation for all the modes at a given time can be evaluated using a binomial test. By comparing the excitation of each mode to ambient noise derived from the same signal and by using a summed-score statistic over both the stations and modes, we have developed a robust statistical test for normal mode excitation.

We apply the technique to the Earth's fundamental spheroidal modes  $s_2$  to  $s_{23}$  as recorded by the IDA network for the entire year 1978. We calculate the level of excitation at 12 hour intervals using a time domain integration technique designed to optimize the signal-to-noise ratio for each mode. The algorithm readily detects teleseismic earthquakes  $M \geq 6$ . Excitation of the lowest frequency modes is most pronounced in previously identified slow earthquakes that occurred in this interval such as the 21 Feb 78 Banda Sea and the 6 Dec 78 Kurile Islands earthquakes. In addition to catalogued earthquakes, there are periods of mode excitation that are not obviously related to any known seismic events. These events may represent earthquakes with slow characteristic rupture velocities that do not generate high-frequency seismic waves. Once such anomalous events are identified they can be characterized using the amplitude and phase of the normal mode peaks, provided signal-to-noise ratio is adequate. The study of earthquakes at extremely low frequencies is complimentary to source studies at higher frequencies and should yield new insight into the earthquake process.

S22-07 1600H

Spectral Scaling Relations for Crustal and Subduction Earthquakes over the Magnitude Range 0 to 7

D. W. A. Taylor Jr and J. A. Snake (Both at: Seismological Observatory, Virginia Polytechnic Institute and State University, Blacksburg, VA 24061) I. S. Sacks and A. T. Lande (Both at: Department of Geological Magnetism, Carnegie Institution of Washington, Washington, DC 20015) T. Takanami (Faculty of Science, Hokkaido University, Sapporo, Japan)

The southeastern corner of Hokkaido Island, Japan is an active seismic region with both crustal and subduction related earthquakes. 10,560 earthquakes have been cataloged by the Hokkaido University network in the period 1974-1986 with epicentral distances of less than 50 km from the Carnegie broadband station KML. The earthquakes range in magnitude from less than -1 to 7 (the Lrakawa-Oka event on 21 March 1982). Based on the seismicity, the top of the subducting Pacific plate enters the study region at about 30 km depth and extends to about 100 km depth on the northwestern edge of the region. For this study two subsets of the events are examined: crustal events and subduction events located within the subducting plate and below 40 km.

Using data from the Carnegie broadband station KML, seismic source scaling relations were derived for 27 shallow events and 25 subduction events. Moments were derived from Q-corrected P, SV and SH amplitude spectra and an average focal mechanism. Corner frequency, radius, and Brune stress drop were determined using the objective technique of Snake (1987, BSSA). Corner frequency and radius are uncorrelated with moment below moments of  $10^{18}$  dyne-cm, and correlated at higher moments. Radius average 0.3 km over the moment range  $10^{18}$  -  $10^{24}$  dyne-cm, with variations of up to a factor of two, and increase from 1 km to over 15 km over the range  $10^{18}$  -  $10^{24}$  dyne-cm. Stress drops are strongly correlated with moment below  $10^{18}$  dyne-cm and uncorrelated for higher moments. For lower moments, stress drops increase with moment from 0.05 bar to 40 bar, and for higher moments, stress drop range from 20 bar to 400 bar, with most values near 100 bar. Moment-magnitude and cepstral analyses indicate that these results are not biased by site effects.

The tectonic stress differs between the interior of the subducting plate and the region above the plate, yet no difference is found between the scaling relations for the crustal earthquakes and the subduction earthquakes taken separately. We conclude, therefore, that the calculated stress drops for smaller events are not primarily a function of the tectonic stress. A model which is consistent with these observations is one in which smaller events result from the failure of an isolated asperity on a preexisting fault. The tectonic stress is taken to be unusual, thus coupling the shear and normal stresses across the fault.

S22-08 1615H

A model of foreshock occurrence with tectonic stress.

J. BREVES-ANDRE (IGPP, University of California, Los Angeles, CA 90024)

A model proposed by Yamashita and Knopoff for foreshock occurrence and intermediate term clustering is modified to include tectonic effects. In the model, we start with an initial three-dimensional random distribution of parallel cracks. Each crack is allowed to grow quasistatically due to stress corrosion at the crack tips. Adjacent cracks will fuse when a predetermined but random value of barrier strength is exceeded. After a long sequence of such fusion events a catastrophic event occurs. The analysis of the stages prior to a main event is carried out as a function of the crack size and gap distribution geometry, the distribution of critical stress, etc. We relate the results of the simulations to ruptures in shallow subduction zones. Some of the factors that influence such an event appear to be the geometry and strengths of the coupling between the cracks, the rate of increase of the external stress field, and the distribution of the asperities.

Extreme Rainfall and Geomorphic Effectiveness II (H22)

Room 102 Tues PM  
Presiding, J. A. Smith  
NOAA/National Weather Service  
R. B. Jacobson  
USGS, Reston

H22-08 1640H

Regulatory Perspective on Geomorphic Stability at Waste Disposal Sites During Extreme Rainfall Events

J. Grimm, T. Johnson and R. J. Starmer (U.S. Nuclear Regulatory Commission, Washington, D.C. 20555; 301-492-0569)

Geomorphic hazards have potential impacts upon the long-term stabilization of inactive uranium mill tailings and low-level radioactive waste. Federal standards address the need for protection of these facilities from two main types of fluvial geomorphic hazards: (1) long-term instability due to processes such as channel changes and gullying, and (2) short-term or sudden instability associated with catastrophic flooding.

NRC staff experience indicates that designs to provide long-term erosion resistance for radioactive waste disposal sites are significantly affected by selection of the design flood event. Reviews by NRC staff of early hydraulic and geomorphic analyses for various disposal sites indicate that a range of statistical assumptions and design strategies are used in determining design basis floods and precipitation events. In addition, predictions of high-magnitude floods are often based on Quaternary stratigraphic studies and paleoflood analyses too limited in scope to use in development of accurate geomorphic criteria for the selection of design events.

Therefore, NRC staff concludes that criteria for long-term stability are met if erosion-protection designs are based on concepts of the Probable Maximum Flood (PMF) and Probable Maximum Precipitation (PMP). The staff conclude that criteria for long-term stabilization may not be met by designs based upon statistically derived flood estimates, limited Quaternary stratigraphic data, or other geomorphic analyses.